Quantum Field-induced Proton H^+ Gradients in Prebiotic Protocell Clusters

Michael Massoth
Department of Computer Science, Hochschule Darmstadt (h_da)
University of Applied Sciences Darmstadt, member of European University of Technology (EUt+)
Darmstadt, Germany
e-mail: michael.massoth@h-da.de

***Abstract*- The origin of the first hydrated proton (H^+) gradients before the rise of biological proton pumps or membrane-bound enzyme complexes remains a central unresolved problem in prebiotic research. Here we show that protocell clusters, formed under saline primordial-soup conditions, are not only stabilized by Casimir–Lifshitz attraction but also generate selective modulation of dynamic Matsubara modes within their nanometer-scale gaps. Because the static mode (n = 0) is fully suppressed by Debye screening, the remaining dynamic modes create geometry-defined resonance zones with lowered vacuum energy. These zones exponentially enrich hydrated protons (H^+) through Casimir–Polder coupling. Dimers act as one-dimensional proton (H^+) channels, while tetrahedral clusters produce three-dimensional proton funnels. The resulting quantum-field-induced proton reservoirs offer a physically plausible precursor to chemiosmotic (H^+) gradients and may have provided the first energetic coupling mechanism between early protocells.**

Keywords-*Casimir–Lifshitz forces; protocell clusters; prebiotic proton gradients; dynamic Matsubara modes; Casimir–Polder potentials; chemiosmotic precursors.*

I. INTRODUCTION

This is the fifth of seven papers on the series: "A Constructivist Proto-Bio-Information Theory: A Physically Grounded Nano-Systems Architecture for Prebiotic Emergence, Information, Proto-Semantic Function, and Sustainability of Protocell Aggregation and Cluster Formation".

Massoth [1] showed that attractive Casimir–Lifshitz forces formed an unavoidable aggregation mechanism under the saline and thermally active conditions of the early Earth. Classical DLVO interactions collapse in the relevant 5–200 nm range [12], while Casimir–Lifshitz attraction remains algebraic, scaling roughly as $1/L^2$, and therefore dominates mesoscale interactions.

Massoth [2] built on this result and demonstrated how these forces generate stable mesoscale protocell clusters, especially dimers and tetrahedra with six loose contact points and typical gap widths of $L \approx 10$ nm. In this nanoregime, Casimir–Lifshitz attraction exceeds thermal energy and suppresses Brownian motion. The outcome is long-lived, geometry-defined protocell clusters that can support both prebiotic energy organization and early, physically implemented information states.

Massoth [3] shows that protocell clusters can generate reproducible differences and functional meaning states. These proto-functional states form the conceptual basis for this paper, where proton gradients appear as early functional signals emerging from physical constraints.

Massoth [4] reveals that Casimir-Lifshitz-shaped resonance zones and ε-machines create syntactic, semantic, and pragmatic layers of early information. This multi-layered framework supports this paper, which interprets proton reservoirs as energetically encoded proto-semantic structures within nanoscale reaction zones.

Structure of the paper: Section II introduces the physical framework of Casimir–Lifshitz–driven protocell clustering and defines the relevant geometric configurations. Section III develops the quantum-field mechanism underlying proton accumulation in nanoscale resonance zones and provides order-of-magnitude estimates. Section IV discusses the prebiotic energetic, informational, and proto-biological implications of these proton reservoirs. Section V concludes with experimental perspectives and directions for future work.

II. QUANTUM-FIELD ORIGINS OF PREBIOTIC PROTON GRADIENTS AND RESEARCH QUESTION

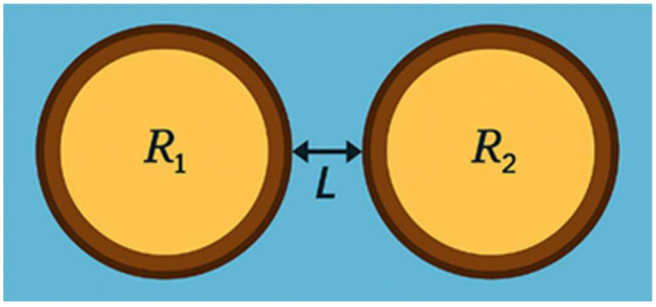

Figure 1. Geometry of a prebiotic protocell dimer

In Figure 1, schematic representation of two spherical protocells with radii R_1 and R_2 separated by a minimal surface-to-surface distance L in saline aqueous solution (primordial soup). This sphere–sphere geometry defines the fundamental configuration used to model Casimir–Lifshitz interactions between protocell membranes under prebiotic conditions.

Energy landscapes were fundamental to the origin of life, yet the emergence of the first proton gradients—long before

biological proton pumps, membrane complexes, or metabolic networks existed—remains a central unresolved question in prebiotic research. Modern chemiosmotic systems rely on complex molecular architectures.

This raises a key research question: could simple protocell assemblies generate proton (H^+) differences [10] from their physical environment and create local energy potentials solely through geometry and the properties of the quantized electromagnetic field?

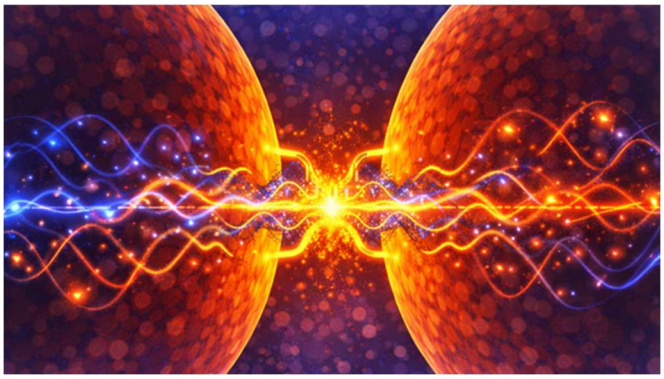

Figure 2. Thermal and quantum vacuum field fluctuations within a nanoscale gap of the prebiotic protocell dimer membranes

This paper explores exactly that scenario [20]. We show that protocell clusters, which can arise spontaneously under prebiotic conditions through Casimir-Lifshitz attraction, induce selective modulation of electromagnetic fluctuations in their nanometer-sized gap regions. Under saline "primordial soup" conditions with ionic strengths of 50–200 mMol, the static Matsubara mode is completely suppressed by Debye screening. As a result, only the fast dynamic modes of the thermal quantum field govern the interaction between cells. These modes create geometry-dependent resonance zones where local vacuum energy is reduced, enabling hydrated protons to accumulate due to their high polarizability.

In Figure 2, two spherical protocells form a narrow intermembrane gap (L= 2-50 nm) in which thermal and quantum electromagnetic fluctuations are geometrically confined. The boundary conditions imposed by the opposing membranes selectively reduce the density of dynamic electromagnetic vacuum modes within the gap. This mode suppression creates a localized minimum of vacuum energy, which gives rise to an attractive Casimir-Lifshitz force that stabilizes the dimer configuration.

The aim of this paper is to develop this quantum-field mechanism systematically and to show that protocell assemblies can generate proton reservoirs solely through their nanoscale structure. These reservoirs serve as plausible precursors to chemiosmotic gradients. This reveals a potentially universal physical process that could have supported early energy provision and functional coupling among protocells, offering a new foundation for prebiotic self-organization and early bioenergetic evolution.

III. The Role of Prebiotic Energetics for Protocells

Bioenergetics is one of life's most universal foundations. All cells use ion gradients—especially proton gradients—to perform work, drive metabolism, and store energy in chemical form. The combined pH gradient (ΔpH) and membrane potential (ΔΨ) form the proton-motive force, which powers ATP synthase and many other processes. This principle is conserved across all domains of life, from bacteria to mitochondria. Proton gradients are therefore a central energetic currency of biology.

This raises a key question in origins-of-life research: how could the first ion gradients arise before specialized membrane proteins, transport channels, or metabolic networks existed? Conventional models often invoke external sources such as geochemical gradients at hydrothermal vents or mineral interfaces. These scenarios provide macroscopic gradients but do not explain how nanoscale, locally stabilized gradients could emerge directly at or between protocells—nor how such gradients could persist long enough to enable early energy conversion rather than dissipating immediately.

Recent proto-physiological work shows that primitive protocells can generate stable ion asymmetries without membrane proteins or transporters. Matveev [24], for example, demonstrated that proteinoid-based model cells can concentrate K^+ ions up to 1600-fold relative to the medium—solely through sorption and phase organization, without pumps or channels. Protocells must therefore be viewed as non-membranous biophysical phases capable of generating electrostatic potentials, selective ion distributions, and energetic nonequilibrium states through their internal structure.

This perspective supports the central thesis of this paper: proton gradients in protocell clusters may not require biological origin. They could arise from the physical structure of vesicle assemblies and their quantum-geometric interactions with electromagnetic fluctuation modes. Protocells could thus have generated physically driven, locally stabilized proton reservoirs long before true proton pumps evolved.

The present paper addresses precisely this research gap. We investigate how quantum- and thermally induced fluctuation forces—specifically Casimir-Lifshitz interactions in saline prebiotic environments—could shape the spatial organization and energetic dynamics of protocells. These forces act at nanometer separations and can determine both stabilization and relative arrangement. In such cluster geometries, the electromagnetic mode spectrum is modified in ways that generate proton fluxes, nanofluidic transport, and local potential minima.

This leads to an alternative view of prebiotic bioenergetics: proton gradients may not be purely biological innovations but emergent products of physical coupling, fluctuation dynamics, and dissipative organization in protocell clusters. For biologists, this suggests that essential elements of chemiosmotic energy conversion may have roots in the physical behavior of simple vesicles. For computer scientists, such gradients illustrate how early protocell assemblies could stabilize and couple states through field structures. For sustainability science, ion gradients appear as early examples of nonequilibrium-driven self-stabilization—a process reflecting core features of prebiotic resilience and energy efficiency.

IV. The Special Geometry of Protocell Clusters

Massoth [2] showed that protocells in prebiotic environments likely did not exist as isolated compartments. Theoretical models and recent experimental analogues indicate that nanoscale vesicles and amphiphile aggregates can spontaneously assemble into clusters in saline solutions through Casimir–Lifshitz attraction. This attraction arises from the reduction of electromagnetic fluctuations in the gap between two membranes and makes certain geometries energetically favored. Two simples, but structurally central clusters emerge: the protocell dimer and the protocell tetrahedron.

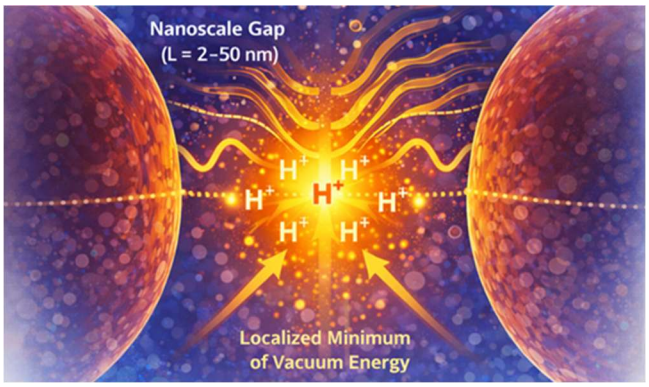

Figure 3. Localized minimum of quantum vacuum energy at the nanoscal gap of the prebiotic protocell dimer spheres with membranes

A dimer forms when two protocells approach within a few nanometers [11]. This produces a well-defined gap region, typically L=2–50 nm [22] wide depending on vesicle size, membrane stiffness, and ionic conditions. This distance lies squarely in the regime where quantum-field mode selection is strongest and dynamic Matsubara modes dominate the electromagnetic field. The intermembrane gap thus acts as a nanoscale resonance cavity that shapes field fluctuations and can generate proton potentials along a one-dimensional axis. Because of their frequency and mechanical stability, dimers represent the simplest and most common form of protocellular cooperation.

In Figure 3, resonance zones emerge in which relevant QED vacuum fluctuations are strongly suppressed. This creates local minima of vacuum energy. Hydrated protons drift passively into these minima and accumulate in a stable manner. Casimir-Lifshitz coupling drives nanoscale quantum-geometric confinement and proton (H^+) enrichment. Attraction between adjacent protocell membranes (L = 2–50 nm) concentrates protons within the intermembrane gap and generates localized electrochemical potentials.

A more structurally influential motif is the protocell tetrahedron—a three-dimensional arrangement of four vesicles whose centers form an almost regular tetrahedron. Such configurations arise when several protocells interact simultaneously through Casimir-Lifshitz attraction. The pairwise gaps again fall within the critical 5–50 nm range, while the center of the tetrahedron becomes a three-dimensional resonance space enclosed by four interfaces. This geometry suppresses selected electromagnetic modes far more strongly than in a dimer, creating a pronounced energetic minimum in the tetrahedral core.

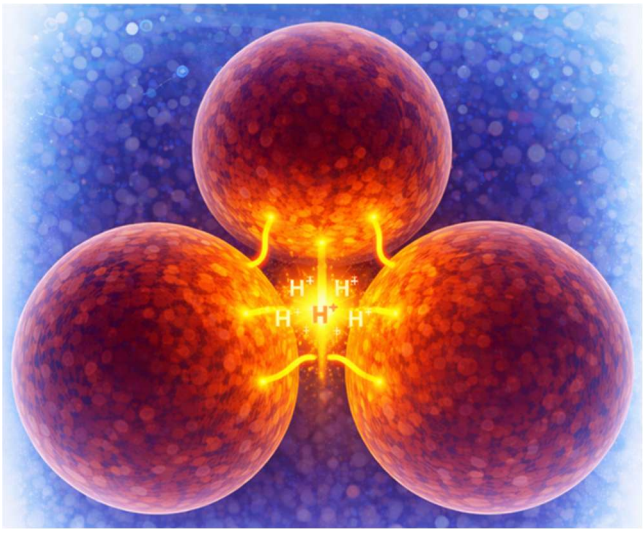

Figure 4. Resonance zone within a protocell tetrahedron

In Figure 4, four protocell spheres (one not visible) with membranes form a tetrahedral geometry. This multi-interface confinement suppresses dynamic vacuum modes and produces a central energy minimum. A three-dimensional resonance zone forms at the geometrical center. The resulting minimum of vacuum energy stabilizes proton (H^+) accumulation within the tetrahedral core. Generating local electrochemical potentials within the resonance zone.

Both geometries—dimer and tetrahedron—are therefore not only energetically preferred but also physically significant. They define the nanoregions in which the electromagnetic field of the primordial environment is most strongly filtered, modulated, and focused. The resulting resonance zones form the foundation for the quantum-field-induced proton reservoirs examined in the following sections.

V. METHODS, NUMERICAL CALCULATIONS AND ORDER-OF-MAGNITUDE VALIDATION

Model Assumptions and Limitations:
These assumptions define a minimal physical model aimed at isolating the contribution of quantum-geometric effects. Protocell radii of 500–1000 nm, intermembrane separation gap L of 2–100 nm, temperatures of 20–80 °C, and ionic strengths of 50–200 mMol define a physically plausible prebiotic parameter window in which Casimir–Lifshitz interactions can contribute to non-chemical mesoscale aggregation. Protocell membranes are treated as smooth dielectric interfaces. Simple fatty-acid membranes exhibit low effective permittivities ($\varepsilon_{membrane} \approx 2–4$), well below that of saline water ($\varepsilon_{water} \approx 75–78$), satisfying the sign condition for attractive Casimir–Lifshitz forces. Protein–membrane-based compartments (PMBCs), with higher effective permittivities ($\varepsilon_{membrane} \approx 3–8$) and increased mechanical stability, are expected to exhibit particularly pronounced and experimentally accessible interactions. Hydrated protons are represented by an effective polarizability, and the electrolyte is described within the linear Debye–Hückel regime. All numerical calculations are obtained using an effective Hamaker constant $A_{eff} = 5 \times 10^{-21}$ Joule, consistent with reported values for membrane–water systems. No active transport, chemical buffering, or metabolic processes are included, and cluster geometries are assumed static on proton diffusion timescales.

Derjaguin proximity-force approximation (PFA):
In the biologically relevant regime $L \ll R$ (here L=2–100 nm and R=500–1000 nm), the exact Casimir–Lifshitz description for a sphere–medium–sphere system can be reduced, via the Derjaguin proximity-force approximation (PFA), to a simple scaling form:

$$F_{CL}(L) \propto A_{eff} R_{eff}/L^2. \quad (1)$$

Here, the effective curvature radius R_{eff} acts as the dominant amplification factor for biological cluster stability [13]. Larger protocells therefore generate systematically stronger coupling at identical material parameters. The following applies:

$$F_{CL}(L) \approx -(A_{eff}/6) * (R_{eff}/L^2) \quad (2)$$
$$\text{with } R_{eff} = (R_1 * R_2)/(R_1 + R_2).$$

Here, A_{eff} denotes an effective Hamaker constant that integrates the spectral dielectric response of the membrane–water system. The force scales linearly with the effective curvature radius R_{eff} and decays algebraically as $1/L^2$.
For the parameter ranges considered below, the resulting potential wells reach several k_BT, making them relevant for mesoscale cluster stabilization.

The corresponding effective binding potential $U_{CL}(L)$ follows directly from integration:

$$U_{CL}(L) \propto -(A_{eff}/6) * (R_{eff}/L), \quad (3)$$

with A_{eff} the membrane–water Hamaker constant, R_{eff} the reduced curvature of the two spheres, and L the minimal surface-to-surface distance. The approximation holds for $L \ll R_i$, L larger than the membrane thickness, and smooth, non-adhesively functionalized interfaces.

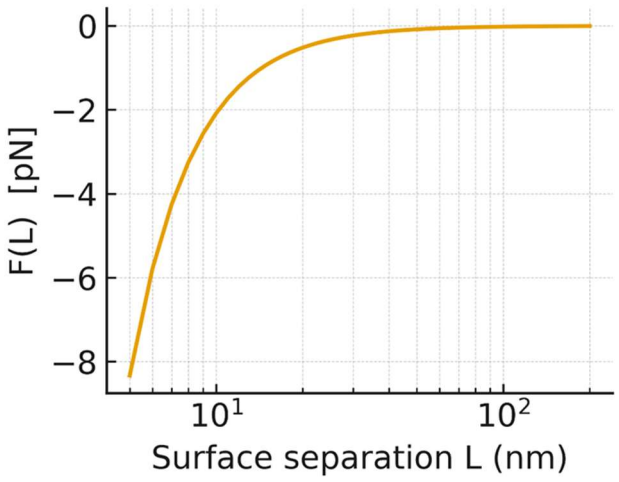

Figure 5. Attractive Casimir–Lifshitz force $F_{CL}(L)$ between two PMBC-like protocells (R_1=R_2=500 nm) as a function of separation L

Figure 5 shows the attractive Casimir‑Lifshitz force $F_{CL}(L)$ between two PMBC-like protocells (R_1=R_2=500 nm) as a function of surface separation L (logarithmic x-axis). The algebraic decay $F_{CL}(L) \propto 1/L^2$ produces significant mesoscale attraction over L=5‑100 nm.

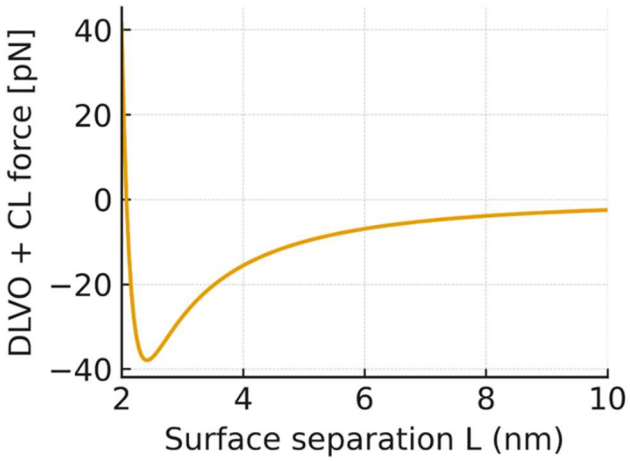

Figure 6. Resulting total force from F_{DLVO} and F_{CL} contributions over L=2–10 nm

Comparison with classical interaction mechanisms: For protocell radii of ~500–1000 nm and separations of ~2–200 nm, a regime emerges in which Casimir–Lifshitz forces become comparable to, or exceed, residual Derjaguin–Landau–Verwey–Overbeek (DLVO) contributions. At prebiotically realistic distances ($L \gtrsim 2$–100 nm), the Casimir–Lifshitz component provides a non-DLVO-compatible, algebraically decaying attraction that persists beyond screened electrostatic interactions. The combined force landscape yields detectable attractive wells (up to ~−38 pN) that stabilize bound protocell configurations against Brownian motion, as calculated and shown in Figure 6. These results indicate that, under saline early-Earth conditions, Casimir–Lifshitz interactions constitute a robust physical aggregation mechanism without requiring universal dominance over classical forces.

VI. Quantum-Physical Derivation of Proton (H^+) Gradients

Proton (H^+) Behavior between two Casimir Plates:
As a first step, consider two parallel Casimir plates immersed in a saline aqueous environment that models a prebiotic soup with ionic strengths of 50–200 mMol. These plates represent protocell membranes or simplified dielectric boundaries. Their separation lies in the nanoscale range (L = 2–100 nm, typically 2–50 nm), where both classical electrostatics and quantum-field-driven Casimir–Lifshitz forces act.
In free vacuum, quantum electromagnetic fluctuations are isotropic. Between two Casimir plates, this symmetry breaks. Only virtual photon modes compatible with the boundary conditions remain allowed. The result is a thinned and shifted spectrum of dynamical vacuum fluctuations.
In an electrolyte, Debye screening adds a second effect. Slow, quasi-static fields are suppressed over 1–2 nm [9]. In Casimir–Lifshitz terms, this eliminates the static thermal Matsubara mode (n = 0) for separations $L \gg 1$–2 nm. Thus only dynamical Matsubara modes ($n \geq 1$) define the effective vacuum field. Their imaginary frequencies are:

$$\xi_n = 2\pi n k_B T/\hbar \text{ with } n \geq 1, \quad (4)$$

where k_B is Boltzmann's constant and T is the temperature.
These modes lie in the far infrared and terahertz range and generate the characteristic quantum dynamic structure in the gap. The resulting field-induced energy density [21] can be written as a sum over the local mode densities $f_n(z)$ at position z:

$$U_{field}(z) \approx k_B T \sum_{n=1}^{\infty} f_n(z), \quad (5)$$

where $f_n(z)$ quantifies the presence of the nth Matsubara mode. Boundary conditions, material properties, and plate separation determine where modes are suppressed. Minima of this potential define quantum-induced resonance zones—regions of reduced vacuum energy and shortened fluctuation spectra.
The dynamical ($n \geq 1$) modes respond sensitively to nanoscale geometry. Because they are not screened in electrolytes, they shape the entire local quantum spectrum. Mode selection acts as a geometric filter that suppresses some field modes while amplifying others. Regions of maximal mode suppression form stable resonance minima with lowered vacuum energy. These minima are robust against thermal noise and produce defined proton reservoirs whose concentrations rise exponentially with the depth of the mode-suppression well.

The key question is how protons (H^+) behave in this quantum-shaped landscape. In water, protons exist as hydrated, highly polarizable clusters [23]. They couple strongly to the fast ($n \geq 1$) Matsubara modes. Their interaction with the modified vacuum field is captured by a Casimir–Polder expression:

$$U_{CP}(z) \approx \frac{1}{2} k_B T \sum_{n=1}^{\infty} \alpha(i\xi n) fn(z), \quad (6)$$

where $\alpha(i\xi_n)$ is the frequency-dependent polarizability of the hydrated proton cluster and $f_n(z)$ the local mode density.
Because $\alpha(i\xi_n) > 0$, protons (H^+) prefer regions where the sum $\sum_{n=1}^{\infty} \alpha(i\xi n) fn(z)$ is minimal [23]: $U_{CP}(z_{min}) = \min_z U_{CP}(z)$.

In symmetric plate–medium–plate systems, this minimum typically lies at the center of the gap, forming a "proton reservoir" without any membrane potential or protein channels.
The stationary proton distribution follows a Boltzmann profile [23]:

$$P(z) \propto \exp[-U_{CP}(z)/k_B T]. \quad (7)$$

Even modest potential shifts of a few $k_B T$ yield exponential proton (H^+) enrichment. For separations of 5–50 nm, the resonance zone accumulates markedly elevated proton concentrations—a quantum-geometric precursor of chemiosmotic gradients.

Interim conclusion: In saline prebiotic media, Debye screening removes the static (n = 0) Matsubara mode. Only dynamical ($n \geq 1$) Matsubara modes contribute to Casimir–Lifshitz forces. These modes shape a spatially varying quantum potential in which protons (H^+) drift toward resonance minima through Casimir–Polder coupling. The result is a purely physical mechanism that generates nanoscale proton (H^+) reservoirs—an early form of prebiotic energy organization.

Proton (H^+) behavior in the reaction zones of protocell dimers and tetrahedra:

Extending the plate model to realistic protocell clusters shows that dimer and tetrahedral configurations strongly structure the accessible electromagnetic fluctuations. Because the n = 0 Matsubara mode is absent under saline conditions, reaction zones are shaped exclusively by the dynamical (n ≥ 1) Matsubara modes. These far infrared and terahertz modes define the local quantum-field landscape for proton (H^+) motion.

As before, the effective proton (H^+) potential is governed by the reduced local mode density $f_n(r)$:

$$U_{CP}(z) \approx \frac{1}{2} k_B T \sum_{n=1}^{\infty} \alpha(i\xi n) fn(z). \quad (8)$$

Resonance zones occur where the mode-suppression term reaches its minimum. Hydrated protons (H^+) respond to these nanoscale potentials according to the Casimir–Polder interaction. Because $\alpha(i\xi_n) > 0$, protons accumulate where fluctuating modes are maximally damped.

Protocell Dimer: One-dimensional Proton (H^+) Guidance

In a dimer, two opposing membranes separated by L form an ordered nanoscale slit. A linear resonance zone develops along the symmetry axis. Dynamical modes (n ≥ 1) are strongly suppressed near the midline, producing a pronounced minimum in $U_{CP}(z)$. The steady-state proton (H^+) distribution obeys:

$$P(z) \propto \exp[-U_{CP}(z)/k_B T]. \quad (9)$$

This creates a one-dimensional proton conduit—a quantum-geometric "proto-proton (H^+) channel" that forms without proteins.

Protocell Tetrahedron: Three-dimensional Resonance Well

In a tetrahedron, modes from four interfaces interfere. Multiple scattering produces deep suppression of specific modes at the center. The resulting potential shows a strong three-dimensional minimum:

$$U_{CP}(\mathbf{r}_{Tetrahedron\text{-}center}) = \min_r U_{CP}(\mathbf{r}). \quad (10)$$

This forms a three-dimensional proton funnel. Proton (H^+) density in the tetrahedral core can exceed the bulk medium outside the tetrahedron cluster by several orders of magnitude:

$$P_{center} / P_{bulk} \propto \exp[\Delta U / k_B T], \quad (11)$$

where ΔU is the depth of the resonance well. Larger ΔU produces exponentially greater proton (H^+) enrichment.

Prebiotic physical implications:

The two geometries generate distinct proton (H^+) landscapes:

- Dimer: directed one-dimensional proton flow
- Tetrahedron: a three-dimensional proton hub

Both structures produce proton (H^+) gradients through geometry and quantum fluctuations alone—a possible physical origin of chemiosmotic organization, predating biological proton pumps.

The total energy of an N-protocell cluster in close contact scales with the number of membrane–membrane bonds N_{bonds} (N):

$$\begin{aligned} E_N(L) &\approx -N_{bonds}(N) * I U_{CL}(L) I \\ &= -N_{bonds}(N) * (A_{eff}/6) * (R_{eff}/L) \\ &= -N_{bonds}(N) * \Lambda(R,L) * k_B T. \end{aligned} \quad (12)$$

For R = 500 nm, L = 10 nm, and $A_{eff} = 5\times10^{-21}$ J, a dimer already binds with ≈ −5.1 $k_B T$, much higher than the thermal noise fluctuations of +1.0 $k_B T$ at ~25 °C.

TABLE I. TOTAL CASIMIR–LIFSHITZ INTERACTION ENERGIES

N	Protocell Structure	N_{bonds}	$E_N/k_B T \approx$
2	Dimer	1	−5.1
3	Triangularer Trimer	3	−15.2
4	Tetrahedron	6	−30.5
6	Oktahedron	12	−61.0
7	Pentagonal Bipyramid	15	−76.2
13	Icosahedral 13-Cluster	42	−213.4

Table I shows the total Casimir–Lifshitz interaction energies $E_N/k_B T$ for representative N-protocell cluster geometries, illustrating how the number of pairwise bonds Nbonds drives mesoscale stabilization.

A potential well of -5 $k_B T$ yields roughly 150-fold proton (H^+) enrichment in a tetrahedral reaction zone. Even such modest depths allow protocells to stabilize reaction sites, catalyze proton-driven processes, support local energy potentials, generate pH differences of 2–3 units, and initiate primitive metabolism-like behavior.

Order-of-magnitude estimate:

The depth of the geometry-induced Casimir–Polder potential well is expected to lie in the range ΔU ≈ 1–5 $k_B T$ for protocell dimers and ΔU ≈ 3–8 $k_B T$ for tetrahedral clusters, depending on the intermembrane separation L and cluster geometry. For narrow gaps (L ≈ 2–10 nm), stronger mode suppression yields ΔU ≈ 3–5 $k_B T$ in dimers and ΔU ≈ 5–8 $k_B T$ in tetrahedra, whereas wider gaps (L ≈ 20–50 nm) correspond to ΔU ≈ 1–3 $k_B T$ and ΔU ≈ 3–5 $k_B T$, respectively. The resulting proton enrichment follows a Boltzmann factor $P_{local}/P_{bulk} \approx \exp(\Delta U/k_B T)$, implying concentration ratios from order-unity up to ~10^2 for dimers and up to ~10^3 for tetrahedra.

These enrichments correspond to local pH shifts of approximately ΔpH ≈ 0.5–2 for dimers and ΔpH ≈ 1–3 for

tetrahedral resonance zones, indicating that nanoscale protocell clusters can sustain biologically relevant proton gradients without active transport mechanisms.

VII. Prebiotic Significance and Implications

The quantum-field-induced proton reservoirs that form in protocell clusters offer a new perspective on prebiotic energetics. Stable proton gradients can arise solely from geometry, polarizability, and thermal quantum fluctuations. Energetic states therefore did not require early biological machines but may have been embedded directly in the physical structure of protocell assemblies. Proton traps in dimers and proton funnels in tetrahedra create local pH centers that promote and stabilize reactions, providing energetic advantages without pumps or membrane proteins.

These mechanisms extend beyond energy supply. In modern cells, proton gradients act not only as energy sources but as key regulatory variables. Quantum-field-based reservoirs may therefore have enabled early self-organization, coordination, and coupling within protocell groups. Dimers would serve as directed energetic channels. Tetrahedra would act as three-dimensional reaction hubs supporting rudimentary metabolic steps. Protocells appear not as isolated compartments but as cooperative micro-assemblies sharing energy and state information through quantum-modulated nanoscale gaps.

The informational implications are similar. Proton gradients in resonance zones can function as early physical memory or state variables, analogous to analog nodes in distributed systems. Their stability and geometric coupling support proto-informational states without polymers or genetic coding. In this sense, energy gradients themselves may represent one of the earliest forms of functional information, consistent with constructor-theoretic ideas.

From a sustainability perspective, these gradients illustrate that core principles of efficient energy systems—generation, storage, controlled dissipation, and resilience—may already have been realized at prebiotic nanoscales. Protocell clusters behave as open dissipative systems that capture energy, structure it, and use it locally. Quantum-field-driven gradient formation thus represents a proto-sustainable organizational mode: a minimal mechanism generating energetic stability in a fluctuating environment without biological infrastructure.

The emergence of quantum-field-induced proton reservoirs transforms protocell clusters from passive aggregates into active energetic systems. By stabilizing localized proton gradients through geometry alone, protocell assemblies acquire functional, non-equilibrium states that persist over biologically relevant timescales. These states represent a physically grounded precursor to chemiosmotic organization and mark a critical step toward proto-living behavior, in which energy, structure, and function become intrinsically coupled.

Overall, these results suggest that early steps toward life were strongly shaped by the capacity of simple protocell assemblies to build quantum-geometrically defined energy structures. Proton reservoirs in the nanoscale gaps of dimers and tetrahedra may have marked the transition from chemistry to proto-biology—a regime in which energy, geometry, and quantum-field structure first merged into functional self-organization.

VIII. Conclusion and Future Work

The results presented here fit into a growing line of research that places physical mechanisms at the center of life's emergence. Classical models of prebiotic energetics often invoke geochemical or molecular gradients. Our analysis shows instead that protocell clusters can become active energetic landscapes themselves. Quantum-field-induced proton reservoirs provide a plausible route toward early chemiosmotic precursors, long before biological proton pumps existed. This offers a physics-based explanation for how early protocells could stabilize their energy budgets and couple to one another.

The underlying mechanisms are experimentally accessible today. Liposome-based model systems can generate nanoscale gaps of L=2–50 nm, where Casimir–Lifshitz forces become measurable. Nanofluidic platforms can resolve proton distributions and pH profiles inside these gaps. Terahertz and infrared spectroscopy can characterize the mode selection of dynamic fluctuations. Together, these tools allow direct tests of the predicted resonance zones and proton traps. Empirical validation of quantum-field-bound energy structures is therefore within reach.

This mechanism does not imply sustained transmembrane chemiosmosis but local, geometry-bound proton reservoirs.

The implications extend beyond origin-of-life studies. In synthetic biology, artificial protocell systems could be engineered to exploit quantum-geometric proton gradients for energy storage, catalytic enhancement, or stabilization of functional states. Such "synthetic protocells" would not rely on biological machines but draw usable energy directly from their physical arrangement. Likewise, the findings point to sustainable nanoscale energy concepts based on dissipative self-organization without external pumping mechanisms.

This work thus highlights a broad research frontier where physics, biology, nanotechnology, and information science converge: the exploration of quantum-geometric energy structures as foundational elements of both prebiotic and synthetic life.

References

[1] M. Massoth, "Attractive Casimir-Lifshitz Forces as a Universal Driver of Prebiotic Protocell Aggregation and Cluster Formation," *BIOTECHNO*, 2026.

[2] M. Massoth, "Emergent Information Formation in Prebiotic Protocell Clusters: A Computational Mechanics Framework of ε-Machines and Attractor Memory," *BIOTECHNO*, 2026.

[3] M. Massoth, "From Physical Difference to Meaning: A Constructor-Theoretic Framework for Prebiotic Information in Casimir–Lifshitz-Coupled Protocell Clusters," *BIOTECHNO*, 2026.

[4] M. Massoth, “Physical Origin of Proto-Information: Syntax, Semantics and Pragmatic Emergence in Prebiotic Protocell Clusters,” *BIOTECHNO*, 2026.

[5] F. E. Rosas, *et al.*, “Software in the natural world: A computational approach to hierarchical emergence,” *arXiv* preprint, 2024, doi:10.48550/arXiv.2402.09090.

[6] M. Deutsch and C. Marletto, “Construction theory of information,” *Proc. R. Soc. A*, vol. 471, art. no. 20140540, 2015, doi:10.1098/rspa.2014.0540.

[7] H. B. G. Casimir, “On the attraction between two perfectly conducting plates,” *Proc. K. Ned. Akad. Wet.*, vol. 51, pp. 793–795, 1948.

[8] E. M. Lifshitz, “The theory of molecular attractive forces between solids,” *Sov. Phys. JETP*, vol. 2, pp. 73–83, 1956.

[9] J. N. Israelachvili, *Intermolecular and Surface Forces*, 3rd ed., Academic Press, London, 2011.

[10] P. C. W. Davies, “Does quantum mechanics play a non-trivial role in life?” *Biosystems*, vol. 78, pp. 69–79, 2004.

[11] I. Gözen, *et al.*, “Protocells: Milestones and recent advances,” *Small*, vol. 18, art. no. 2106624, 2022.

[12] S. K. Lamoreaux, “Demonstration of the Casimir force in the 0.6–6 μm range,” *Phys. Rev. Lett.*, vol. 78, pp. 5–8, 1997.

[13] J. L. Garrett, D. A. T. Somers, and J. N. Munday, “Measurement of the Casimir force between two spheres,” *Phys. Rev. Lett.*, vol. 120, art. no. 040401, 2018.

[14] P. Rodriguez-Lopez, “Casimir energy and entropy in the sphere–sphere geometry,” *Phys. Rev. B*, vol. 84, art. no. 075431, 2011.

[15] S. J. Rahi, T. Emig, N. Graham, R. L. Jaffe, and M. Kardar, “Scattering theory approach to electrodynamic Casimir forces,” *Phys. Rev. D*, vol. 80, art. no. 085021, 2009.

[16] G. Bimonte and T. Emig, “Exact results for classical Casimir interactions: Dirichlet and Drude model in the sphere–sphere and sphere–plane geometry,” *Phys. Rev. Lett.*, vol. 109, art. no. 160403, 2012.

[17] A. Canaguier-Durand, G.-L. Ingold, M.-T. Jaekel, A. Lambrecht, P. A. Maia Neto, and S. Reynaud, “Classical Casimir interaction in the plane–sphere geometry,” *Phys. Rev. A*, vol. 85, art. no. 052501, 2012.

[18] B. B. Machta, S. L. Veatch, and J. P. Sethna, “Critical Casimir forces in cellular membranes,” *Phys. Rev. Lett.*, vol. 109, art. no. 138101, 2012.

[19] D. S. Ether, I. S. Nogueira, and H. M. Nussenzveig, “Probing the Casimir force with optical tweezers,” *Europhys. Lett.*, vol. 112, art. no. 44001, 2015.

[20] S. Pei, Z. Zhang, T. Li, *et al.*, “Direct measurement of the van der Waals force between a pair of microspheres based on photonic force microscopy,” *Opt. Eng.*, vol. 60, art. no. 084101, 2021.

[21] M. Boström and B. E. Sernelius, “Thermal effects on the Casimir force in the 0.1–5 μm range,” *Phys. Rev. Lett.*, vol. 84, pp. 4757–4760, 2000.

[22] H.-J. Butt, “Measuring electrostatic, van der Waals, and hydration forces in electrolyte solutions with an atomic force microscope,” *Biophys. J.*, vol. 60, pp. 1438–1444, 1991.

[23] S. Cukierman, “Et tu, Grotthuss! And other unfinished stories,” *Biochim. Biophys. Acta*, 2006, doi:10.1016/j.bbabio.2005.12.001.

[24] V. V. Matveev, “Comparison of fundamental physical properties of the model cells (protocells) and living cells reveals the need for protophysiology,” *Int. J. Astrobiol.*, vol. 16, no. 1, pp. 97–106, 2017, doi:10.1017/S1473550415000476.